

*Supporting Information for:*

# Proton Coupled Electron Transfer from the Excited State of a Ruthenium(II) Pyridylimidazole Complex

*Andrea Pannwitz, Oliver S. Wenger\**

Department of Chemistry, University of Basel, St. Johannis-Ring 19, CH-4056 Basel, Switzerland

## Table of content

1	Synthesis.....	2
2	Equipment and methods .....	2
3	[Ru(bpy) <sub>2</sub> pyimH] <sup>2+</sup> .....	4
3.1	Electronic absorption and ground-state acidity constant (pK <sub>a</sub> ) of [Ru(bpy) <sub>2</sub> pyimH] <sup>2+</sup> .....	4
3.2	Luminescence and excited-state acidity constant (pK <sub>a</sub> <sup>*</sup> ) of [Ru(bpy) <sub>2</sub> pyimH] <sup>2+</sup> .....	5
3.3	Cyclic voltammetry of [Ru(bpy) <sub>2</sub> pyimH] <sup>2+</sup> .....	7
3.4	Spectro-electrochemistry of [Ru(bpy) <sub>2</sub> pyimH] <sup>2+</sup> .....	8
3.5	Effect of buffer concentration on excited-state properties of [Ru(bpy) <sub>2</sub> pyimH] <sup>2+</sup> .....	9
4	Monoquat (MQ <sup>+</sup> ) .....	10
4.1	Electronic absorption and pK <sub>a</sub> of MQ <sup>+</sup> .....	10
4.2	Cyclic voltammetry of MQ <sup>+</sup> .....	11
5	PCET from the excited state.....	12
5.1	Photoproducts .....	12
5.1.1	Decay of photoproducts at pH 2 .....	12
5.1.2	Decay of photoproducts at pH 13 .....	12
5.1.3	Formation of photoproducts at pH 6.3.....	13
5.1.4	Formation of photoproducts in unbuffered H <sub>2</sub> O / CH <sub>3</sub> CN and D <sub>2</sub> O / CH <sub>3</sub> CN mixture at pH/pD 7.3 .....	14
5.2	Stern-Volmer experiments with MQ <sup>+</sup> .....	15
5.2.1	Stern-Volmer luminescence quenching experiment at pH 2 .....	15
5.2.2	Stern-Volmer experiment at pH 13 .....	16

5.2.3	Stern-Volmer experiment at pH 6.3 .....	17
5.2.4	Stern-Volmer experiment in unbuffered water/acetonitrile.....	18
5.2.5	Stern-Volmer experiment in unbuffered deuterium oxide/acetonitrile .....	19
6	References .....	20

## 1 Synthesis

All commercially available chemicals for synthesis were used as received. The ligand 2-(2-pyridyl)imidazole (pyimH) was synthesized from 2-pyridinecarbonitrile.<sup>[1]</sup> The RuCl<sub>2</sub>(bpy)<sub>2</sub> precursor complex was prepared from RuCl<sub>3</sub>·3H<sub>2</sub>O and 2,2'-bipyridine.<sup>[2]</sup> The synthesis of [Ru(bpy)<sub>2</sub>pyimH]<sup>2+</sup> from RuCl<sub>2</sub>(bpy)<sub>2</sub> and pyimH was reported previously by Haga and coworkers.<sup>[3]</sup> Cl<sup>-</sup> to PF<sub>6</sub><sup>-</sup> anion exchange was performed according to a previously published method.<sup>[4]</sup>

*N*-methyl-4,4'-bipyridinium (MQ<sup>+</sup>) was synthesized from 4,4'-bipyridine and iodomethane. MQ<sup>+</sup> was precipitated and isolated as a hexafluorophosphate salt.<sup>[5]</sup>

## 2 Equipment and methods

Acetonitrile for electrochemical and photophysical measurements was HPLC grade, and water had Millipore standard. Salts for buffers were used as received and aqueous buffer solutions (0.1 M concentration) were prepared according to standard procedures.<sup>[6]</sup> The following buffers were used for the various pH ranges: TsOH / TsONa (pH 1.0-2.0), citric acid (pH 2.2-3.6), acetate (pH 3.6-5.6), phosphate (pH 5.8-8.0), glycine / NaOH (pH 8.6-10.6), phosphate (pH 11.0-12.0). To obtain pH 13, NaOH was used. Unless otherwise noted all measurements were performed in deaerated 1:1 (v:v) CH<sub>3</sub>CN / H<sub>2</sub>O with 0.05 M buffer concentration at 25 °C.

The pH of the solvent mixture was determined by correcting the measured pH<sup>meas</sup> in the mixture by using the relationship  $\text{pH} = \text{pH}^{\text{meas}} - \delta$ . For the 1:1 (v:v) CH<sub>3</sub>CN / H<sub>2</sub>O mixture the correction constant  $\delta$  is -0.257.<sup>[7]</sup> All pH values reported in the main paper were corrected accordingly.

Cyclic voltammetry was performed on a Versastat3-200 potentiostat from Princeton Applied Research using a glassy carbon disk working electrode. A Standard calomel electrode served as reference electrode, and a platinum wire was used as a counter electrode. In the electrochemical experiments, 0.05 M buffer served as supporting electrolyte. Prior to voltage sweeps at rates of  $0.1 \text{ V s}^{-1}$  the solution was flushed with argon.

UV-Vis spectra were measured on a Cary 5000 instrument from Varian.

Steady-state luminescence experiments were performed on a Fluorolog-3 apparatus from Horiba Jobin-Yvon using an excitation wavelength of 474 nm. Luminescence lifetime and transient absorption experiments occurred on an LP920-KS spectrometer from Edinburgh Instruments equipped with an iCCD from Andor. The excitation source was the frequency-doubled output from a Quantel Brilliant b laser. For aerated optical spectroscopic experiments, quartz cuvettes from Starna and Helma were used. For all deaerated optical spectroscopic experiments the samples were de-oxygenated via three subsequent freeze-pump-thaw cycles in home-built quartz cuvettes that were specifically designed for this purpose.

The following experimental errors were taken into account by the determination of every parameter:

Lifetimes are accurate to 10 %, ground state redox potentials are accurate to  $\pm 0.05 \text{ V}$ .

For values that were obtained from data fitting we report the standard deviation resulting from the respective fits. The errors of not directly measurable values were calculated by error propagation (eq. S1)

$$\Delta z = \sum_{i=1}^n \left( \left| \frac{\partial y}{\partial x_i} \right| \cdot \Delta x_i \right) \quad (\text{eq. S1})$$

### 3 [Ru(bpy)<sub>2</sub>pyimH]<sup>2+</sup>

#### 3.1 Electronic absorption and ground-state acidity constant (pK<sub>a</sub>) of

#### [Ru(bpy)<sub>2</sub>pyimH]<sup>2+</sup>

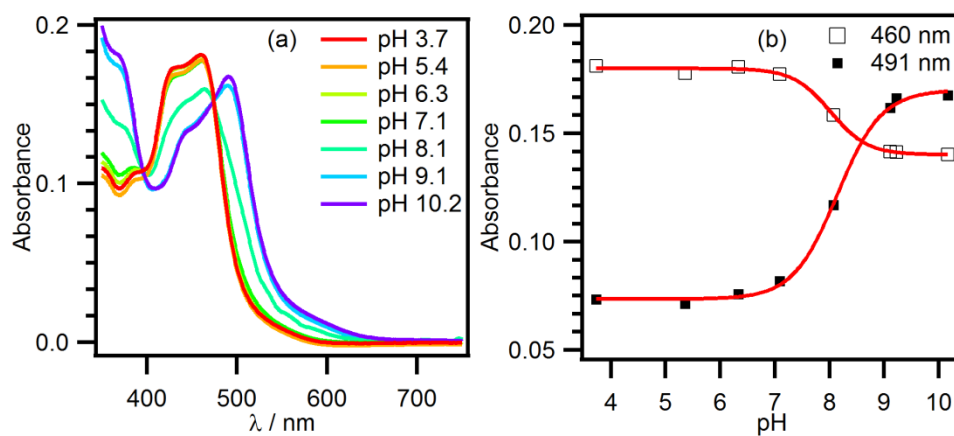


**Figure S1** (a) UV-Vis absorption spectra of 43 μM [Ru(bpy)<sub>2</sub>pyimH]<sup>2+</sup> in 1:1 (v:v) CH<sub>3</sub>CN / H<sub>2</sub>O at different pH values, (b) absorbance at (□) 460 and (■) 491 nm as a function of pH. The red curves are fits.

Fits to the experimental absorbance vs. pH values yields inflection points at  $\text{pK}_a^{460} = 8.02 \pm 0.05$  and  $\text{pK}_a^{491} = 8.14 \pm 0.05$ . Based on these two values we determine a ground-state acidity constant (pK<sub>a</sub>) of  $8.1 \pm 0.1$ .

### 3.2 Luminescence and excited-state acidity constant ( $\text{pK}_a^*$ ) of $[\text{Ru}(\text{bpy})_2\text{pyimH}]^{2+}$

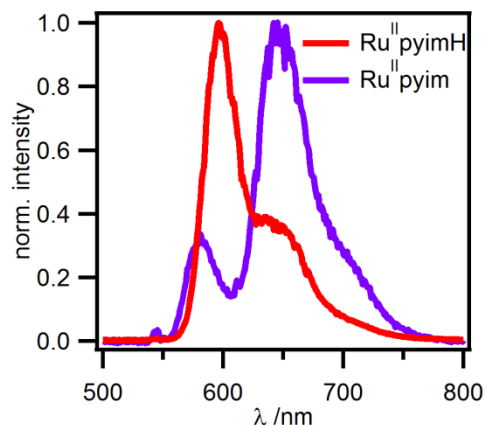


**Figure S2** Normalized luminescence spectra of  $[\text{Ru}(\text{bpy})_2(\text{pyimH})]^{2+}$  (red) and  $[\text{Ru}(\text{bpy})_2(\text{pyim})]^+$  (purple) in 4:1 (v:v) ethanol / methanol at 77 K after excitation at 474 nm.

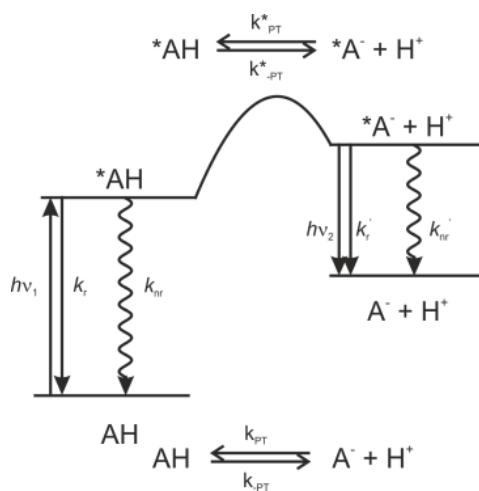


**Figure S3** Dissociation of a generic acid AH in ground (bottom) and electronic excited states (top). Schematic illustration of the thermodynamics associated with photoacid behavior and relevant excited-state decay processes.<sup>[8]</sup>

According to the Förster equation, the relationship between acidity constants in electronic ground ( $\text{pK}_a$ ) and excited states ( $\text{pK}_a^*$ ) is described by:<sup>[8]</sup>

$$\text{pK}_a^* = \text{pK}_a - \frac{h\Delta\nu}{2.3 k T} \quad (\text{eq. S2})$$

$$\text{pK}_a^* = \text{pK}_a - \frac{hc}{2.3 kT} \left( \frac{1}{\lambda_1} - \frac{1}{\lambda_2} \right) \quad (\text{eq. S3})$$

At 25 °C the emission band maxima are  $\lambda_1 = (625 \pm 5)$  nm and  $\lambda_2 = (675 \pm 5)$  nm (see main article). Based on equation S3, the excited-state acidity constant ( $\text{pK}_a^*$ ) is therefore  $5.3 \pm 0.6$ .

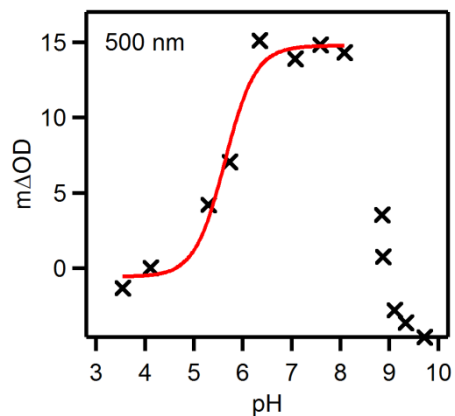


**Figure S4** pH-dependent transient absorption changes ( $\Delta\text{OD}$ ) at 500 nm of 40  $\mu\text{M}$   $[\text{Ru}(\text{bpy})_2\text{pyimH}]^{2+}$  in 1:1 (v:v)  $\text{CH}_3\text{CN} / \text{H}_2\text{O}$  with 0.05 M buffer concentration after excitation with laser pulses of  $\sim 10$  ns duration at 532 nm and integration over the first 200 ns. The red fit curve exhibits an inflection point ( $\text{pH}_i$ ) at  $5.6 \pm 0.2$ .

### 3.3 Cyclic voltammetry of $[\text{Ru}(\text{bpy})_2\text{pyimH}]^{2+}$

The data shown in Figure S5 were used to establish the Pourbaix diagram shown in Figure 1b of the main paper.

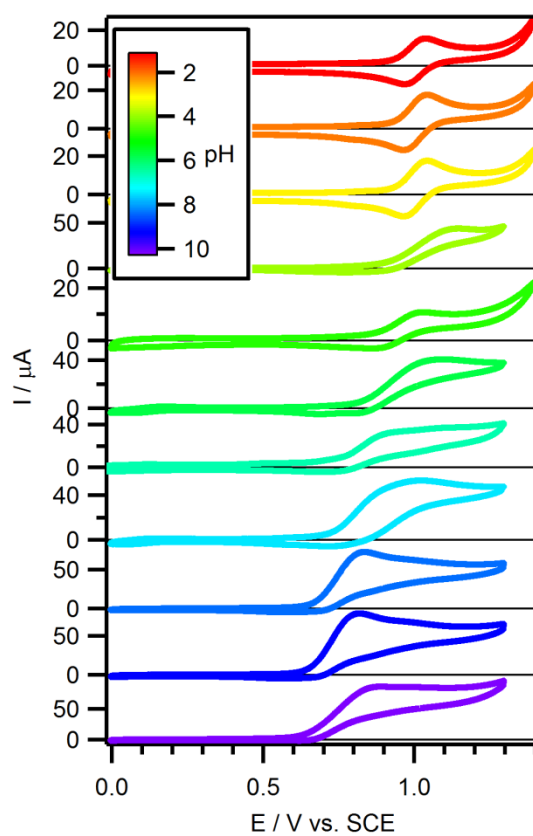


**Figure S5** Oxidation waves of  $[\text{Ru}(\text{bpy})_2\text{pyimH}]^{2+}$  1:1 (v:v)  $\text{CH}_3\text{CN} / \text{H}_2\text{O}$  at different pH values. 0.05 M buffer was used as supporting electrolyte and to adjust the pH.

### 3.4 Spectro-electrochemistry of $[\text{Ru}(\text{bpy})_2\text{pyimH}]^{2+}$

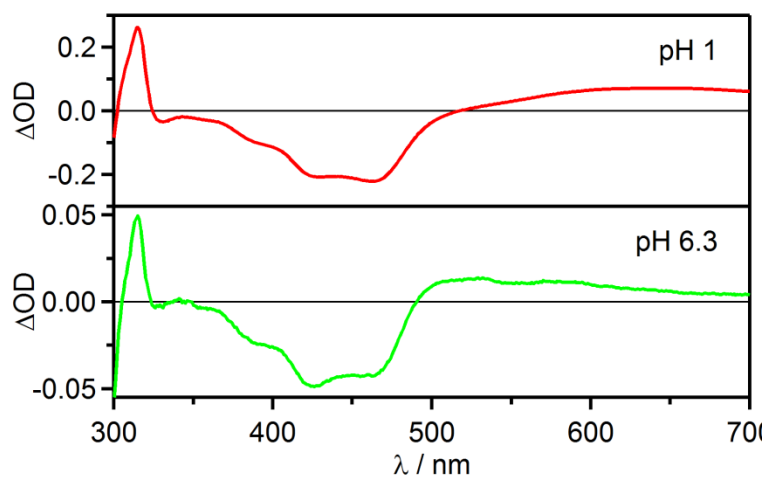


**Figure S6** Spectro-electrochemical UV-Vis difference spectra recorded from a 40  $\mu\text{M}$  solution of  $[\text{Ru}(\text{bpy})_2\text{pyimH}]^{2+}$  in 1:1 (v:v)  $\text{CH}_3\text{CN} / \text{H}_2\text{O}$ , following application of a potential of 1.0 V vs. SCE. The UV-Vis spectrum prior to application of any potential served as a baseline. 0.05 M buffer was used as supporting electrolyte.

### 3.5 Effect of buffer concentration on excited-state properties of $[\text{Ru}(\text{bpy})_2\text{pyimH}]^{2+}$

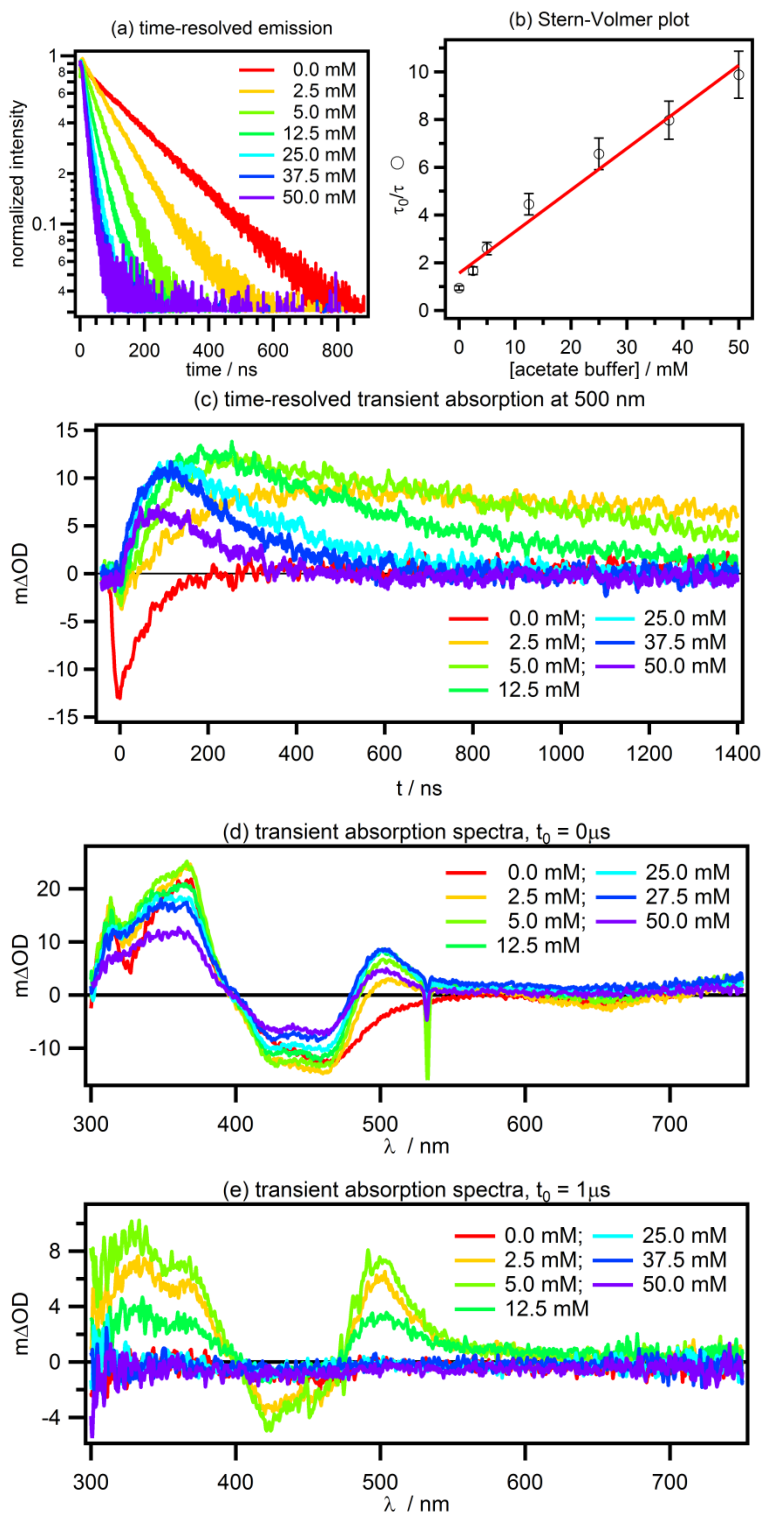


**Figure S7.** Luminescence of  $30\ \mu\text{M}$   $[\text{Ru}(\text{bpy})_2\text{pyimH}]^{2+}$  in buffered 1:1  $\text{CH}_3\text{CN}/\text{H}_2\text{O}$  (v:v) at pH 6.3 as a function of acetic acid/sodium acetate buffer concentration. (a) Kinetic emission at 630 nm after excitation with laser pulses of  $\sim 10$  ns duration at

532 nm, Stern-Volmer plot based on the time-resolved emission data from (a). (c) Change in optical density at 500 nm as a function of time after excitation at 532 nm. (d, e) Transient absorption spectra recorded with a delay of (d) 0  $\mu$ s and (e) 1  $\mu$ s after excitation with laser pulses of  $\sim$ 10 ns duration at 532 nm. Spectra were time-integrated over a period of 200 ns.

## 4 Monoquat (MQ<sup>+</sup>)

### 4.1 Electronic absorption and pK<sub>a</sub> of MQ<sup>+</sup>

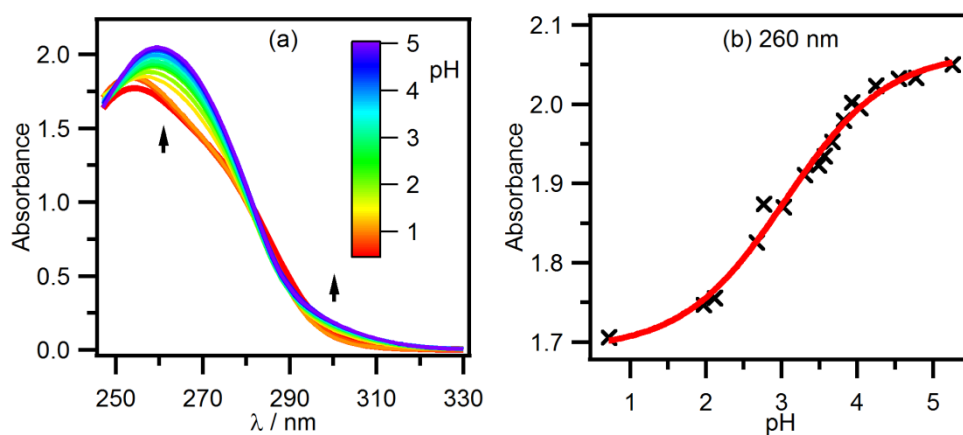


**Figure S8** (a) UV-Vis spectra of MQ<sup>+</sup> in 1:1 (v:v) CH<sub>3</sub>CN / H<sub>2</sub>O as a function of pH; (b) absorbance at 260 nm vs. pH. The red fit curve has its inflection point at pK<sub>a</sub> = 3.0 ± 0.3. HCl and 0.05 M citric acid buffer were used for pH adjustment in this range

## 4.2 Cyclic voltammetry of $\text{MQ}^+$

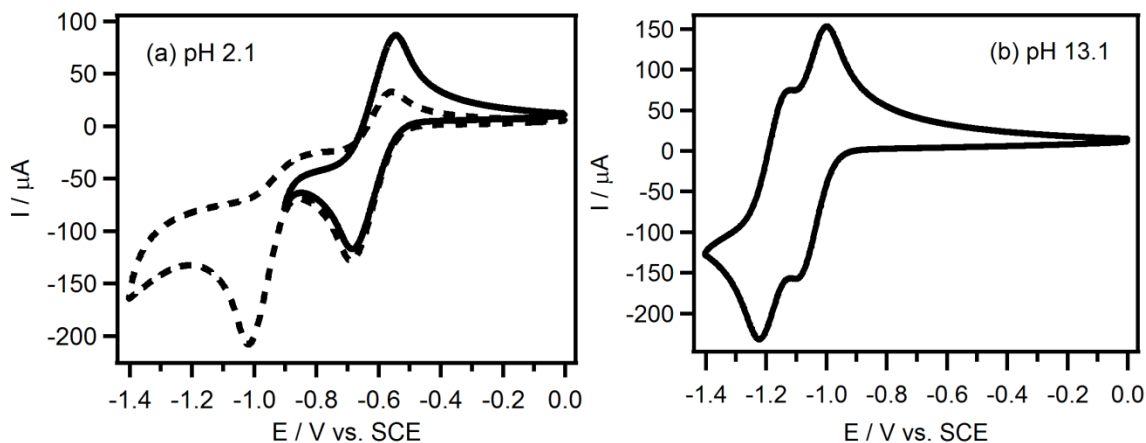


**Figure S9** Cyclic voltammograms (CVs) of  $\text{MQ}^+$  in 1:1 (v:v)  $\text{CH}_3\text{CN} / \text{H}_2\text{O}$ . (a) Reduction waves at pH 2.1; solid line: reduction wave for the  $\text{HMQ}^{2+}/\text{HMQ}^{\bullet+}$  couple, dashed line: reduction waves for the  $\text{MQH}^{2+}/\text{MQH}^{\bullet+}$  and  $\text{HMQ}^{\bullet+}/\text{HMQ}$  couples. (b) reduction waves for the  $\text{MQ}^+/\text{MQ}^{\bullet}$  and the  $\text{MQ}^{\bullet}/\text{MQ}^-$  couples at pH 13.1.

	$E_1$ [V vs. SCE]	$\Delta E_1$ [V]	$E_2$ [V vs. SCE]	$\Delta E_2$ [V]
<b>pH 2.1</b>	$-0.61 \pm 0.05$	0.14	$-1.0 \pm 0.1$ (irrev.)	-
<b>pH 13.1</b>	$-1.06 \pm 0.05$	0.11	$-1.18 \pm 0.05$	0.09

**Table S1** Electrochemical potentials for the first and second reduction  $E_1$  ( $\text{MQH}^{2+}/\text{MQH}^{\bullet+}$  at pH = 2.1 and  $\text{MQ}^+/\text{MQ}^{\bullet}$  at pH = 13.1) and  $E_2$  ( $\text{HMQ}^{\bullet+}/\text{HMQ}$  at pH = 2.1 and  $\text{MQ}^{\bullet}/\text{MQ}^-$  at pH = 13.1) and separations of oxidative and reductive peak potentials  $\Delta E_1$  and  $\Delta E_2$ .

## 5 PCET from the excited state

### 5.1 Photoproducts

#### 5.1.1 Decay of photoproducts at pH 2

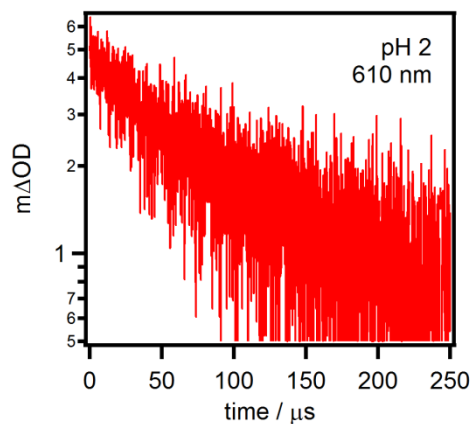


**Figure S10** Decay of the transient absorption signal at 610 nm in the reaction of 30  $\mu\text{M}$   $[\text{Ru}(\text{bpy})_2\text{pyimH}]^{2+}$  with 60 mM  $\text{MQ}^+$  in 1:1 (v:v)  $\text{CH}_3\text{CN} / \text{H}_2\text{O}$  at pH 2. These data monitor the decay of  $\text{HMQ}^{\bullet+}$  to  $\text{HMQ}^{2+}$ , following selective excitation of the metal complex at 532 nm with laser pulses of  $\sim 10$  ns duration.

#### 5.1.2 Decay of photoproducts at pH 13

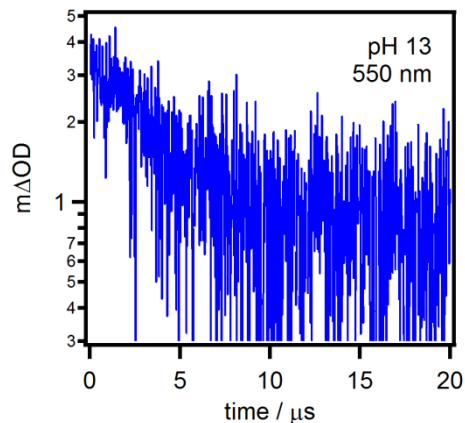


**Figure S11** Decay of the transient absorption signal at 550 nm in the reaction of 30  $\mu\text{M}$   $[\text{Ru}(\text{bpy})_2\text{pyimH}]^{2+}$  with 60 mM  $\text{MQ}^+$  in 1:1 (v:v)  $\text{CH}_3\text{CN} / \text{H}_2\text{O}$  at pH 13. The decay of  $\text{MQ}^{\bullet}$  to  $\text{MQ}^+$  is monitored at this wavelength.

### 5.1.3 Formation of photoproducts at pH 6.3

In the main article the kinetics for the reaction of photoexcited  $[\text{Ru}(\text{bpy})_2\text{pyimH}]^{2+}$  with monoquat in presence of 5 mM acetate buffer was discussed.

The following time constants were obtained in presence of 50 mM buffer concentration for the same reaction:

$^3\text{MLCT}$  lifetime:  $(18 \pm 2)$  ns

formation of  $\text{HMQ}^{\bullet+}$ :  $(50 \pm 5)$  ns

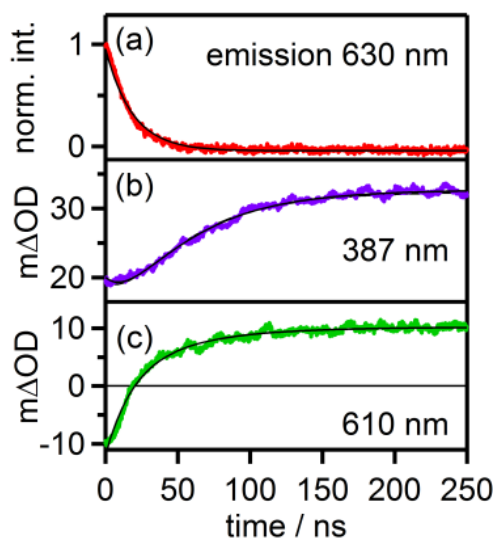


**Figure S12** (a) Temporal evolution of the emission signal at 630 nm and of the transient absorption signals at 387 nm (b) and 610 nm (c) in the reaction of  $[\text{Ru}(\text{bpy})_2\text{pyimH}]^{2+}$  with 60 mM  $\text{MQ}^+$  in 1:1 (v:v)  $\text{CH}_3\text{CN} / \text{H}_2\text{O}$  at pH 6.3 with 0.05 M acetate buffer. Black traces are (a) monoexponential and (b,c) biexponential fits yielding the abovementioned time constants.

### 5.1.4 Formation of photoproducts in unbuffered H<sub>2</sub>O / CH<sub>3</sub>CN and D<sub>2</sub>O / CH<sub>3</sub>CN mixture at pH/pD 7.3

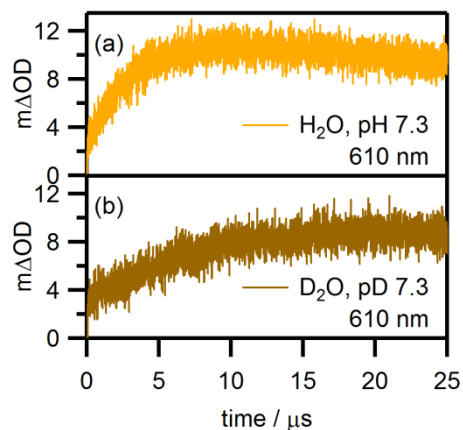


**Figure S13** Temporal evolution of the transient absorption signal at 610 nm in the photo-reaction of 50  $\mu\text{M}$   $[\text{Ru}(\text{bpy})_2\text{pyimH}]^{2+}$  with 60 mM  $\text{MQ}^+$  in unbuffered (a) 1:1 (v:v)  $\text{CH}_3\text{CN} / \text{H}_2\text{O}$  at pH 7.3 and (b) in 1:1 (v:v)  $\text{CH}_3\text{CN}/\text{D}_2\text{O}$  at pD 7.3. This detection wavelength monitors the formation and decay of  $\text{HMQ}^{*+}$ . Excitation occurred at 532 nm. (a) fit with an  $\text{A} \rightarrow \text{B} \rightarrow \text{C}$  reaction kinetics model, yielded  $\tau^{\text{A} \rightarrow \text{B}} = (2.5 \pm 0.3) \mu\text{s}$  for the protonation of  $\text{MQ}^\bullet$  to  $\text{HMQ}^{*+}$  and  $\tau^{\text{B} \rightarrow \text{C}}$  in the order of  $(2.0 \pm 0.2) \mu\text{s}$ , (b) fit according to saturation kinetics for the formation of  $\text{DMQ}^{*+}$  yielded  $\tau^{\text{A} \rightarrow \text{B}} = (6.5 \pm 0.7) \mu\text{s}$ .

## 5.2 Stern-Volmer experiments with MQ<sup>+</sup>

### 5.2.1 Stern-Volmer luminescence quenching experiment at pH 2

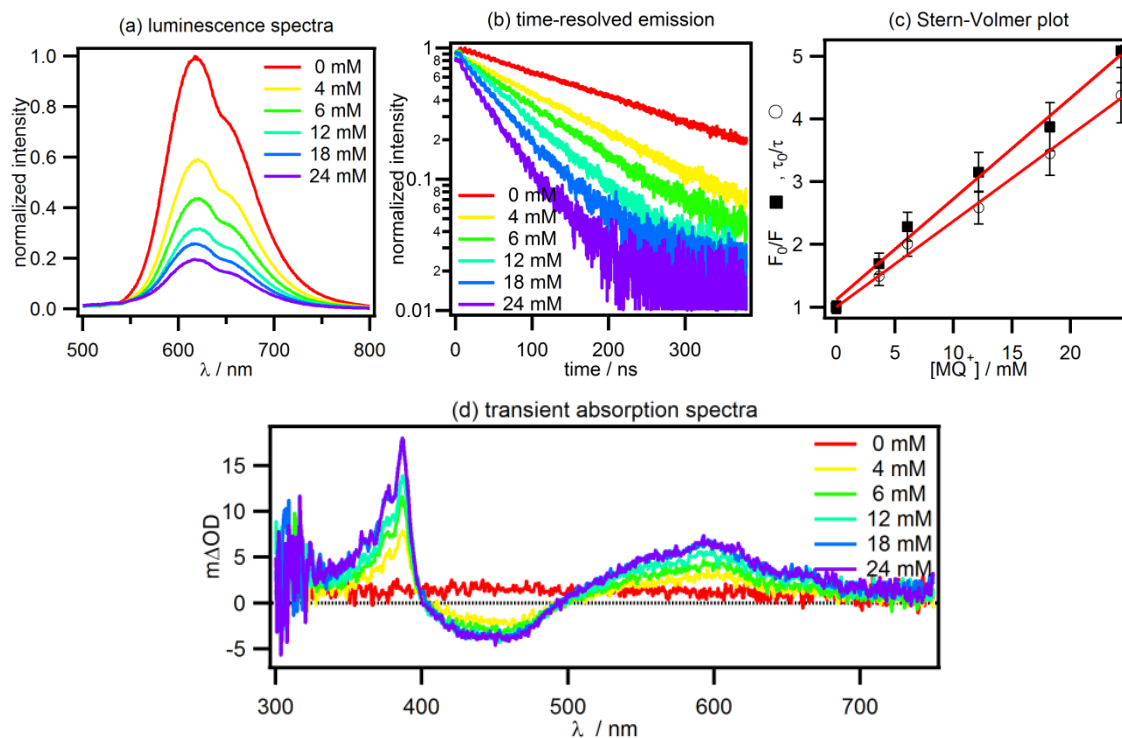


**Figure S14** (a) Luminescence spectra of 20 μM [Ru(bpy)<sub>2</sub>pyimH]<sup>2+</sup> in 1:1 (v:v) CH<sub>3</sub>CN / H<sub>2</sub>O at pH 2 in presence of various MQ<sup>+</sup> concentrations. Excitation occurred at 474 nm. (b) Decay of the emission at 660 nm after excitation with laser pulses of ~10 ns duration at 532 nm. (c) Stern-Volmer plots based on the steady-state luminescence and kinetic emission data from (a) and (b). (d) Transient absorption spectra recorded with a delay of 2 μs after excitation with laser pulses of ~10 ns duration at 532 nm. Spectra were time-integrated over a period of 200 ns.

### 5.2.2 Stern-Volmer experiment at pH 13

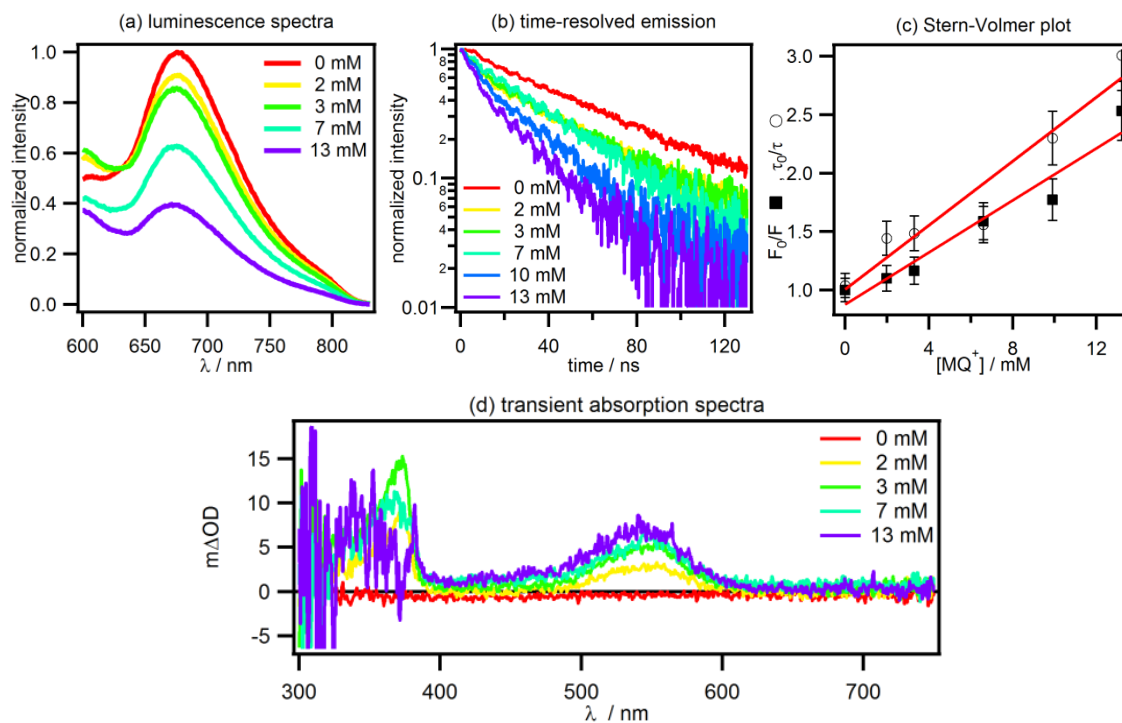


**Figure S15** Luminescence of  $20 \mu\text{M}$   $[\text{Ru}(\text{bpy})_2\text{pyimH}]^{2+}$  in 1:1  $\text{CH}_3\text{CN} / \text{H}_2\text{O}$  (v:v) at pH 13 as a function of  $\text{MQ}^+$  concentration. (a) Steady-state luminescence spectra after excitation at 474 nm. (b) Decay of the emission at 660 nm after excitation with laser pulses of  $\sim 10$  ns duration at 532 nm. (c) Stern-Volmer plots based on the steady-state luminescence and time-resolved emission data from (a) and (b). (d) Transient absorption spectra recorded with a delay of  $2 \mu\text{s}$  after excitation with laser pulses of  $\sim 10$  ns duration at 532 nm. Spectra were time-integrated over a period of 200 ns.

### 5.2.3 Stern-Volmer experiment at pH 6.3

In the following, complementary transient absorption spectra for the experiment at lower buffer concentration 5 mM.

A-B-C kinetics were fitted according to equation S5:

$$f(x) = y_0 + \frac{1}{\tau_1} A \left\{ \left[ \exp\left(\frac{-(x-x_0)}{\tau_1}\right) - \exp\left(\frac{-(x-x_0)}{\tau_2}\right) \right] \left[ \frac{\tau_2^{-1} - \tau_1^{-1}}{\tau_1^{-1} - \tau_2^{-1}} \right]^{-1} \right\} \quad (\text{eq. S5})$$

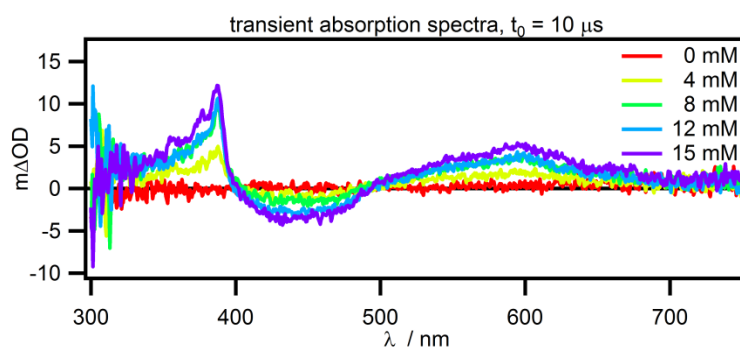


**Figure S16** Transient absorption spectra obtained after photo-excitation of 40 μM [Ru(bpy)<sub>2</sub>pyimH]<sup>2+</sup> in 1:1 (v:v) CH<sub>3</sub>CN / H<sub>2</sub>O containing 5 mM acetate buffer at pH 6.3 in presence of different MQ<sup>+</sup> concentrations. Transient absorption spectra were recorded with a delay of 10 μs after excitation with laser pulses of ~10 ns duration at 532 nm. Spectra were time-integrated over a period of 200 ns.

## 5.2.4 Stern-Volmer experiment in unbuffered water/acetonitrile

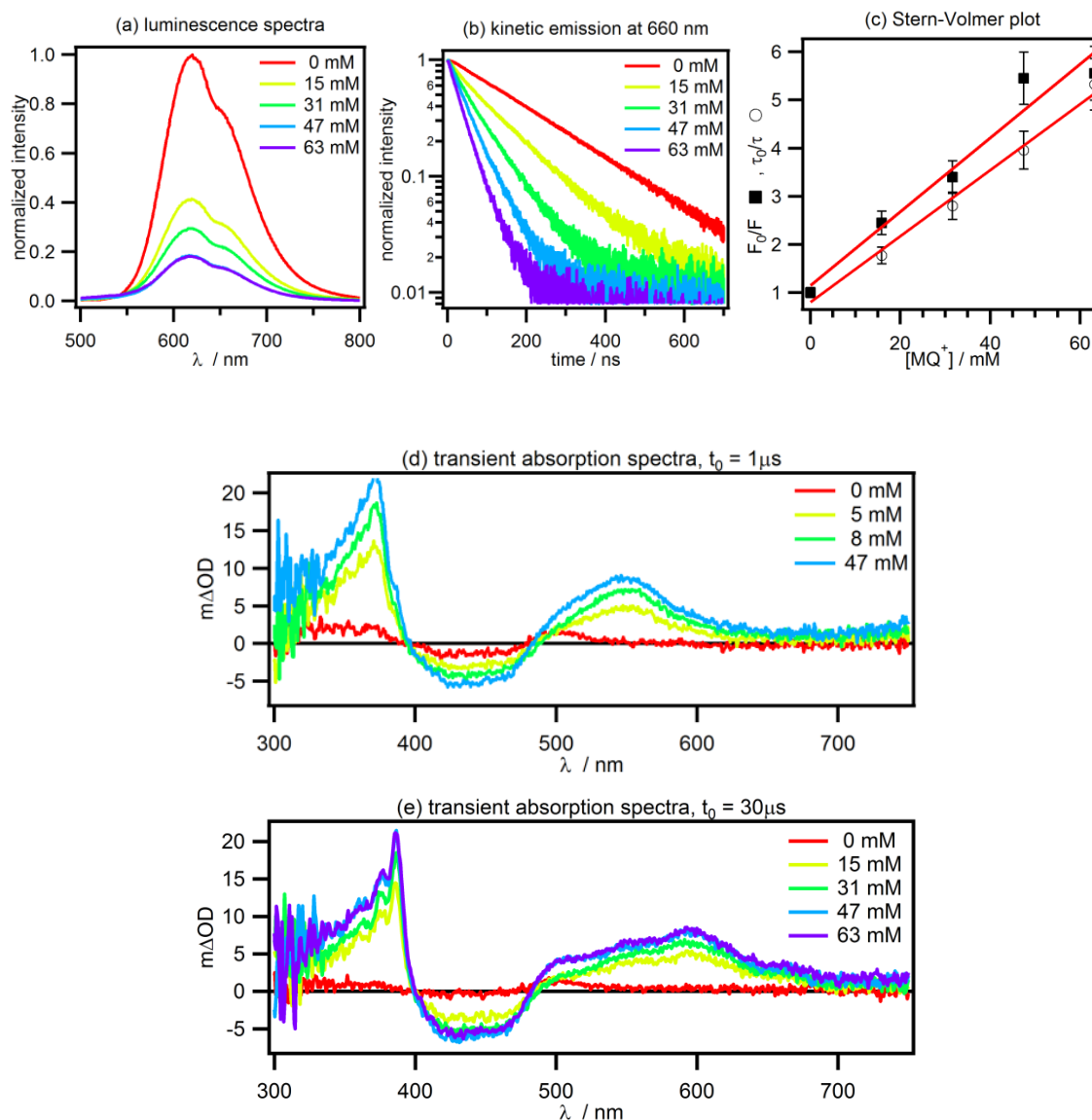


**Figure S17** Luminescence of  $40 \mu\text{M}$   $[\text{Ru}(\text{bpy})_2\text{pyimH}]^{2+}$  in unbuffered  $1:1 \text{ CH}_3\text{CN} / \text{H}_2\text{O}$  (v:v) at pH 7.3 as a function of  $\text{MQ}^+$  concentration. (a) Steady-state luminescence spectra after excitation at 474 nm, (b) time-resolved emission at 660 nm after excitation with laser pulses of  $\sim 10$  ns duration at 532 nm, (c) Stern-Volmer plots based on the steady-state luminescence and time-resolved emission data from (a) and (b). (d, e) Transient absorption spectra recorded with a delay of (d)  $1 \mu\text{s}$  and (e)  $30 \mu\text{s}$  after excitation with laser pulses of  $\sim 10$  ns duration at 532 nm. Spectra were time-integrated over a period of 200 ns.

### 5.2.5 Stern-Volmer experiment in unbuffered deuterium oxide/acetonitrile

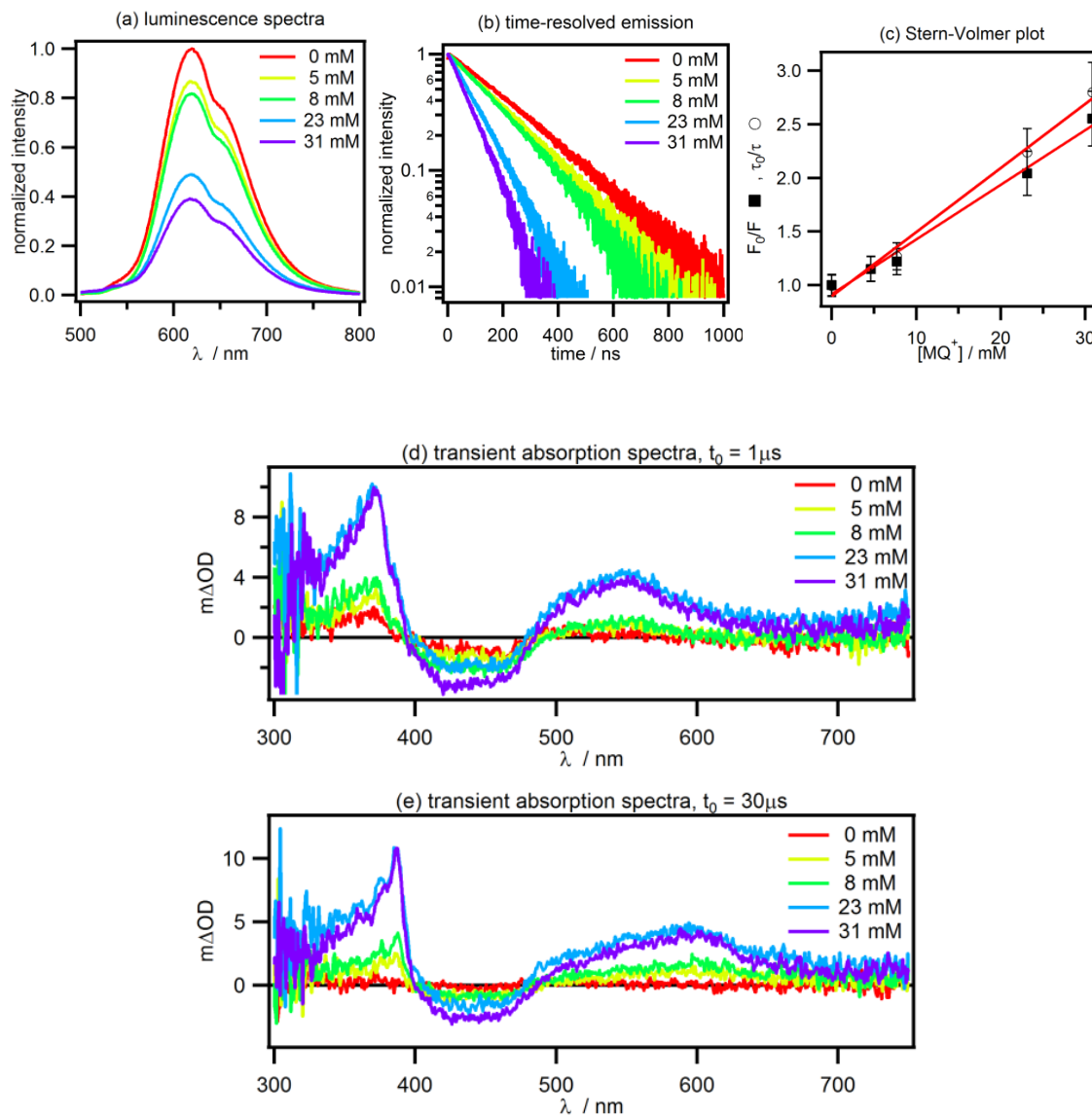


**Figure S18.** Luminescence of  $20 \mu\text{M}$   $[\text{Ru}(\text{bpy})_2\text{pyimH}]^{2+}$  in unbuffered  $1:1 \text{ CH}_3\text{CN}/\text{D}_2\text{O}$  (v:v) at pH 7.3 as a function of  $\text{MQ}^+$  concentration. (a) Steady state luminescence spectra after excitation at 474 nm. (b) Kinetic emission at 660 nm after excitation with laser pulses of  $\sim 10$  ns duration at 532 nm, (c) Stern-Volmer plots based on the steady-state luminescence and kinetic emission data from (a) and (b). (d, e) Transient absorption spectra recorded with a delay of (d)  $1 \mu\text{s}$  and (e)  $30 \mu\text{s}$  after excitation with laser pulses of  $\sim 10$  ns duration at 532 nm. Spectra were time-integrated over a period of 200 ns.

## 6 References

- [1] M. E. Voss, C. M. Beer, S. A. Mitchell, P. A. Blomgren, P. E. Zhichkin, *Tetrahedron* **2008**, *64*, 645–651.
- [2] B. P. Sullivan, D. J. Salmon, T. J. Meyer, *Inorg. Chem.* **1978**, *17*, 3334–3341.
- [3] M.-A. Haga, *Inorg. Chim. Acta* **1983**, *75*, 29–35.
- [4] K. M. Lancaster, J. B. Gerken, A. C. Durrell, J. H. Palmer, H. B. Gray, *Coord. Chem. Rev.* **2010**, *254*, 1803–1811.
- [5] D. J. Feng, X. Q. Li, X. Z. Wang, X. K. Jiang, Z. T. Li, *Tetrahedron* **2004**, *60*, 6137–6144.
- [6] D. D. Perrin, B. Dempsey, *Buffers for pH and Metal Ion Control*, Chapman And Hall, London, **1979**.
- [7] L. G. Gagliardi, C. B. Castells, C. Ràfols, M. Rosés, E. Bosch, *Anal. Chem.* **2007**, *79*, 3180–3187.
- [8] L. M. Tolbert, K. M. Solntsev, *Acc. Chem. Res.* **2002**, *35*, 19–27.